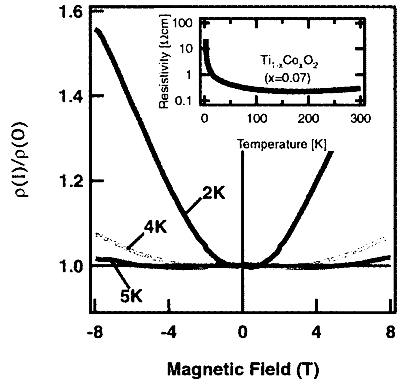

Fig. 4. The MR measurements of the $x = 0.07$ specimen in the temperature range of 2 to 5 K. A positive MR = 60% is observed at 2 K in a field of 8 T applied normal to the surface. The temperature dependence of the resistivity is also shown (inset).

Assuming that thermal equilibrium is reached in our growth conditions, the valence state of Co ions should be either Co^{2+} or Co^{3+}, in view of the facts that the films were deposited at 950 to 1000 K and cooled down to 500 K in 1×10^{-6} to 1×10^{-5} torr of oxygen (*16*). If Co ions are in high spin state, we expect S to vary from 3/2 to 4/2, depending on the mixing ratio of Co^{2+} and Co^{3+} in the film, giving a spontaneous magnetic moment m_{sp} between 3 and 4 μ_B/Co. Meanwhile, the low spin states of Co^{2+} and Co^{3+} yield at most $S = 1/2$ ($m_{sp} = 1$ μ_B/Co). The low spin configuration of Co ions is thus consistent with the observed magnetic moment in the M-H curve in Fig. 3A. In other words, the ferromagnetism of Co-TiO_2 is attributable to the local spins of Co ions.

X.-D. Xiang and co-workers reported magnetoresistance but not ferromagnetism in a class of $LnMCoO_3$ (Ln = Y or La; M = Sr, Ca, or Ba) (*17*). The anatase structure can be viewed as a stacking of TiO_2 B-site layers along the c axis in perovskite. From the viewpoint of this structural similarity between $LnMCoO_3$ and Co-doped TiO_2, the origins of these two magnetic effects may be related. The results reported here are rather serendipitous, and the underlying microscopic mechanism of long-range order is still an open question at present.

References and Notes

1. H. Ohno, *Science* **281**, 951 (1998).
2. J. K. Furdyna, *J. Appl. Phys.* **64**, R29 (1998).
3. T. Fukumura, Z. W. Jin, A. Ohtomo, H. Koinuma, M. Kawasaki, *Appl. Phys. Lett.* **75**, 3366 (2000).
4. K. Sato, H. K. Yoshida, *Jpn. J. Appl. Phys.* **39**, L555 (2000).
5. Z. W. Jin *et al.*, in preparation.
6. H. Kim *et al.*, *Appl. Phys. Lett.* **69**, 25 (1996).
7. A. Fujishima, K. Honda, *Nature* **238**, 37 (1972).
8. L. Forro *et al.*, *J. Appl. Phys.* **75**, 633 (1994).
9. Y. Matsumoto *et al.*, *SPIE Proc.* **3941**, 19 (2000).
10. M. Murakami *et al.*, in preparation.
11. Y. Matsumoto *et al.*, *Jpn. J. Appl. Phys.* **38**, L603 (1999).
12. O. Chauvet, L. Forro, I. Kos, M. Miljak, *Solid State Commun.* **93**, 667 (1995).
13. R. Wolfe, A. J. Kurtzig, R. C. LeCraw, *J. Appl. Phys.* **41** (no. 3), 1218 (1970).
14. J. Q. Xiao, J. S. Jiang, C. L. Chien, *Phys. Rev. Lett.* **68**, 3749 (1992).
15. S. Mitani, H. Fujimori, S. Ohnuma, *J. Magn. Magn. Mater.* **165**, 141 (1997).
16. M. W. Chase Jr. *et al.*, *J. Phys. Chem. Ref. Data* **14**, suppl. no. 1 (1985).
17. G. Briceño *et al.*, *Science* **270**, 273 (1995).

18. The authors express their thanks for financial support from the Comet project of Science and Technology Agency in Japan as well as from the Japan Society for the Promotion of Science.

28 September 2000; accepted 18 December 2000
Published online 11 January 2001; 10.1126/science.1056186
Include this information when citing this paper.

First Solvation Shell of the Cu(II) Aqua Ion: Evidence for Fivefold Coordination

Alfredo Pasquarello,[1,2*] Ingrid Petri,[3] Philip S. Salmon,[3]
Olivier Parisel,[1,2] Roberto Car,[1,4] Éva Tóth,[5] D. Hugh Powell,[6]
Henry E. Fischer,[7] Lothar Helm,[5] André E. Merbach[5]

We determined the structure of the hydrated Cu(II) complex by both neutron diffraction and first-principles molecular dynamics. In contrast with the generally accepted picture, which assumes an octahedrally solvated Cu(II) ion, our experimental and theoretical results favor fivefold coordination. The simulation reveals that the solvated complex undergoes frequent transformations between square pyramidal and trigonal bipyramidal configurations. We argue that this picture is also consistent with experimental data obtained previously by visible near-infrared absorption, x-ray absorption near-edge structure, and nuclear magnetic resonance methods. The preference of the Cu(II) ion for fivefold instead of sixfold coordination, which occurs for other cations of comparable charge and size, results from a Jahn-Teller destabilization of the octahedral complex.

Copper is one of the most abundant transition elements in biological systems, with an occurence of 80 to 120 mg in a normal human body (*1*), but the behavior of its simplest aqueous form, the Cu(II) ion, remains poorly understood. Because of its electronic d^9 configuration, a Jahn-Teller distortion is generally assumed to axially elongate two bonds of the octahedral $[Cu(H_2O)_6]^{2+}$ complex (*2–15*), yielding an unusually fast water exchange rate (*13*, *15*). In addition, an even shorter time scale has been observed and has been attributed to rapid transformations between configurations differing by the orientation of the elongation (*14*, *15*). However, validation of this model suffers from the experimental difficulties associated with measuring the axial Cu-O bond lengths (*2–12*)

The nearest-neighbor Cu-O bond lengths in aqueous solution are well characterized by a variety of experimental techniques such as x-ray diffraction (*2–4*), extended x-ray absorption fine structure (EXAFS) (*5–9*), x-ray absorption near-edge structure (XANES) (*7*, *8*), and isotopic substitution in neutron diffraction (*10–12*), all of which provide consistent values in the 1.94 to 2.00 Å range. By contrast, the more distant axial bond lengths have so far eluded accurate determination, as manifested by the large interval over which the measured values are spread (2.12 to 2.60 Å) (*12*). These problems stem at least partly from the fact that x-ray diffraction, EXAFS, and XANES measurements all require fitting procedures that incorporate a priori assumptions about the structure (*2–9*) and that first-difference pair distribution functions obtained by neutron diffraction cannot discern axial Cu-O from overlapping Cu-H correlations (*10–12*).

We have undertaken a combined experimental and theoretical investigation to unveil the detailed structure and dynamics of the hydrated Cu(II) complex in aqueous solution. We applied the second-difference isotopic substitution method in neutron diffraction

---

[1] Institut Romand de Recherche Numérique en Physique des Matériaux (IRRMA), PPH-Ecublens, CH-1015 Lausanne, Switzerland. [2] Ecole Polytechnique Fédérale de Lausanne (EPFL), PPH-Ecublens, CH-1015 Lausanne, Switzerland. [3] Department of Physics, University of Bath, Bath BA2 7AY, UK. [4] Department of Chemistry and Princeton Materials Institute, Frick Chemical Laboratory, Washington Road, Princeton University, Princeton, NJ 08544, USA. [5] Institut de Chimie Minérale et Analytique, Université de Lausanne, Bâtiment de chimie, CH-1015 Lausanne-Dorigny, Switzerland. [6] Department of Chemistry, Durham University, Durham DH1 3LE, UK. [7] Laboratoire pour l'Utilisation du Rayonnement Electromagnétique (LURE), Bâtiment 209d, Centre Universitaire Paris-Sud, Boîte Postale 34, F-91898 Orsay Cédex, France.

*To whom correspondence should be addressed. E-mail: Alfredo.Pasquarello@epfl.ch

(*16*, *17*) to find the location of the more distant O atoms. In this method, the diffraction patterns measured for solutions differing only by their isotopic composition are combined to give separately the pair distribution functions $g_{CuO}(r)$ and $g_{CuH}(r)$, which describe the average location of, respectively, oxygen and hydrogen atoms relative to the Cu(II) ion. First-principles molecular dynamics simulations (*18–20*), which account for the critical interplay between electronic structure and atomic motions, support the experimental results and reveal the atomic dynamics within the hydrated complex.

Two solutions containing 2.0 molal $Cu(ClO_4)_2$ and 0.1 molal $DClO_4$ in D_2O were prepared with ^{65}Cu and ^{63}Cu isotopes (99% enrichment) (*21*). Two similar solutions with H replacing D were prepared with concentrations ensuring the same atomic fractions as in the deuterated solutions: $1Cu^{2+}:2ClO^{-}_{4}:25(H/D)_2O:0.05(H/D)ClO_4$. Raman and nuclear magnetic resonance (NMR) measurements indicate that the perchlorate ions in aqueous solutions are not prone to inner-sphere complexing (*7*). Taking crystallographic data for $Cu(ClO_4)_2 \cdot 6H_2O$ into consideration (*22*), we deduce that, in solution, distances between the Cu(II) ion and the O and Cl atoms of the perchlorate ions are larger than 3.85 and 4.50 Å, respectively. Similarly, Cu-Cu distances are expected to be larger than 5.14 Å.

Two first-difference functions, one for the deuterated and the other for the hydrogenated solutions, were obtained by subtracting the measured diffraction patterns for the solutions with different Cu isotopes (*23*). The first-difference function extracted for the deuterated solutions closely agrees with previous results (*10*). Neglecting differences in quantum motions, we assume structural isomorphism for hydrogen and deuterium. The two first-difference functions can then be combined to extract (Fig. 1) the partial pair distribution function $g_{CuH}(r)$ (*16*, *17*), as well as the function

$$\Delta G(r) = g_{CuO}(r) + 0.044 g_{CuCu}(r) + 0.102 g_{CuCl}(r) \quad (1)$$

which represents a linear combination of partial pair distribution functions with coefficients resulting from the concentrations and neutron scattering lengths of the species in our solutions. The function $\Delta G(r)$ reduces to $g_{CuO}(r)$ at distances below 4.50 Å, where Cu-Cl and Cu-Cu correlations are not expected to occur (*7*, *22*). To assess the effect of statistical noise, the reciprocal space data were smoothed using a spline fitting method and a minimum noise method. The difference between the coordination numbers obtained with the two procedures provides an error estimate of ±0.15 and ±0.20 for the Cu-O and Cu-H correlations, respectively.

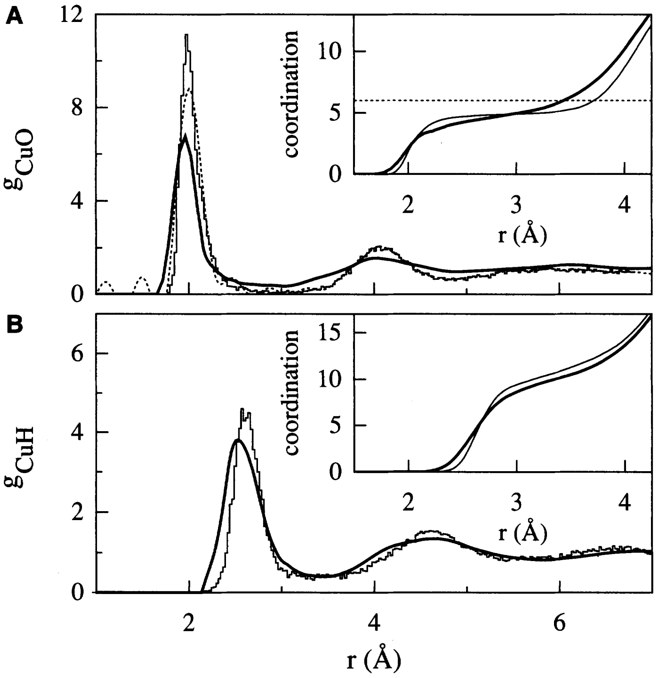

Fig. 1. Partial pair correlation functions $g_{CuO}(r)$ (**A**) and $g_{CuH}(r)$ (**B**) obtained by the second-difference isotopic substitution method in neutron diffraction (thick curves) and by first-principles molecular dynamics (thin curves). The experimental $g_{CuO}(r)$ corresponds to $\Delta G(r)$ given in Eq. 1. The dotted curve in (A) corresponds to the theoretical $g_{CuO}(r)$ obtained by considering the same momentum transfer range as in the experiment (*23*). The coordination numbers as a function of cutoff radius are given in the insets. The horizontal dashed line (inset, upper panel) corresponds to sixfold oxygen coordination.

In the region of the first solvation shell ($r < 3.0$ Å), $g_{CuO}(r)$ shows a single peak at 1.96 Å (Fig. 1), with no definite signature for elongated bonds. A fivefold coordination is achieved by integration up to 3.02 Å, with the sixth O atom situated in the 3.02 to 3.44 Å range. Because O atoms beyond 3.0 Å are generally not considered to be bonded (*24*), this strongly suggests fivefold coordination. The distribution function $g_{CuH}(r)$ corroborates this picture. The first peak occurs at 2.54 Å and gives a coordination number of 8 at 2.89 Å, with the four more distant H atoms distributed over a wide range extending up to 3.80 Å. At the first minimum of $g_{CuH}(r)$ at 3.41 Å, a coordination number of 10.0 is measured.

The molecular dynamics simulations (*18–20*) were carried out using a periodically repeated system consisting of a single Cu^{2+} ion and 50 water molecules (*25*). Extensive test runs at 300 K showed negligible diffusion at this temperature, yielding glassy structural configurations. We selected one of these configurations, in which the Cu(II) ion was fourfold coordinated, for starting the molecular dynamics. During a time period of about 6 ps, we varied the temperature between 300 and 380 K while monitoring the diffusion. We then fixed the temperature at 350 K, where the diffusion rate showed liquidlike behaviour. Within 1 ps of this regime, the Cu(II) ion became fivefold coordinated and maintained this coordination state for the remainder of the simulation (17 ps). A time period of 16 ps, during which the Cu(II) ion was fivefold coordinated, was taken for statistical averages. To test our theoretical approach, we also simulated a Ni(II) ion under identical conditions as the Cu(II) ion. In agreement with the experiment (*16*, *26*), we obtained sixfold coordination validating our method. We then selected one sixfold-coordinated configuration and replaced Ni(II) with Cu(II). When the simulation was restarted, fivefold coordination of the Cu(II) ion was recovered within 1 ps.

The theoretical pair distribution functions show excellent agreement with the experiment for all the principal features (Fig. 1). Despite the higher temperature in the simulation, the theoretical features are found to be sharper than in the experiment. The largest difference is observed for the first peak in the $g_{CuO}(r)$ function. A substantial part of this difference results from the finite momentum transfer range measured in the experiment (*23*) (Fig. 1). Residual differences in peak heights and the adjustment by 50 K on the thermal scale should be attributed to the finite size of the simulation cell (*27*), to the neglect of quantum motions of the H nuclei, and to intrinsic limitations of the generalized gradient approximation (*28*, *29*). Such a small thermal adjustment is not expected to affect the primary solvation number of the Cu(II) ion (*30*), because relevant activation energies of divalent transition-metal ions in aqueous solution typically range between 10 and 60 kJ/mol (*31*) and are thus substantially larger than 0.4 kJ/mol, the energy that corresponds to a temperature of 50 K.

The simulations permit an analysis of the structural configurations. In spite of the thermal fluctuations, we could identify the out-of-plane Cu-O bond by adopting a geometrical criterion, namely the absence of a trans in-plane ligand at approximately 180°. This enabled us to define the stereochemistry of the fivefold-coordinated

Cu(II) ion in terms of the parameter τ (Fig. 2), which describes the in-plane angular distortions by representing the percentage of trigonal distortion of a square pyramidal configuration (*24*). During the simulation, the hydrated Cu(II) complex was found to undergo structural transformations known as Berry twists (*24*), as illustrated by the evolution of τ. Starting from a square-pyramidal–like configuration, the complex transformed around time $t = 16$ ps to a trigonal-bipyramidal–like configuration. Several unsuccessful transition attempts could also be discerned. During the simulation, the structural parameters of the hydrated Cu(II) complex (such as the bond lengths, the parameter τ, and the out-of-plane displacement of the Cu^{2+} ion) were found to vary in a correlated way following the same empirical rules that were derived for crystalline structures (*24*). This provides support for the stereochemical behavior of the fivefold-coordinated Cu(II) ion in our simulation.

Experimental data obtained by nondiffractive methods have previously been invoked to support a sixfold-coordinated Cu(II) ion. Here we specifically address visible near-infrared absorption (*26*), XANES (*7*), and NMR (*15*) measurements and argue that the results can be reinterpreted in terms of a fivefold-coordinated Cu(II) ion.

The visible near-infrared spectrum of Cu(II) aqueous solutions (*26*) shows a broad peak centered at about 1.5 eV (Fig. 3, inset). To test whether this is consistent with fivefold coordination, we calculated the joint density between the relevant filled and empty *d* states. We took an average over seven instantaneous atomic configurations in the simulation, representing a broad range of τ (Fig. 3). For comparison, we also calculated such a density of states for a $[Cu(H_2O)_6]^{2+}$ cluster with a chosen tetragonal elongation of 0.2 Å. The two calculated spectra are essentially indistinguishable once allowance is made for thermal broadening in the cluster calculation. This suggests that transition energies are not substantially affected by the different bonding hybridizations in the five- and sixfold-coordinated Cu(II) complex. Despite the neglect of transition matrix elements and excitonic effects, the calculated densities of states also show a fair agreement with the experimental absorption spectrum (*26*).

To examine the compatibility of the measured XANES spectrum (*7*) with fivefold coordination of the Cu(II) ion, we calculated the XANES spectrum associated with our simulation. For an individual atomic configuration, a spectrum was obtained by considering the density of empty states of *p* symmetry in the core region of the Cu(II) ion. The theoretical XANES spectrum results from an average over eight atomic configurations, equally spaced in time. The correspondence between the theoretical and the experimental spectra fully supports fivefold coordination of the Cu(II) ion (Fig. 4).

The limited length of our simulation does not allow us to predict the water exchange rate with the bulk of the liquid or the relative frequencies of occurrence of square-pyramidal–like and trigonal-bipyramidal–like configurations. Nevertheless, the above results suggest the following picture for the dynamics in the first solvation shell of the Cu(II) aqua ion. The fivefold coordination and its fluctuation between different configurations of the hydrated Cu(II) complex facilitate the water exchange process and provide an explanation for its fast rate (*15*). Furthermore, the high attempt rate in the evolution of τ (Fig. 2) suggests that the typical time scale of Berry twists lies in the picosecond range. This provides a mechanism affecting the magnetic relaxation of the ^{17}O nuclei in the Cu(II) hydration shell and is consistent with the short time scale (~5 ps) observed in NMR experiments (*15*). Indeed, the ^{17}O NMR data (*15*) can successfully be reinterpreted in terms of a fivefold-coordinated

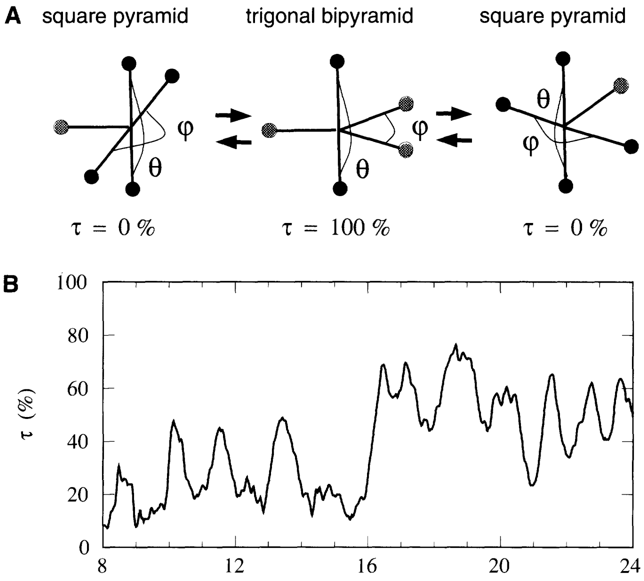

Fig. 2. Evolution of the parameter $\tau = (\theta - \varphi)/60 \times 100\%$, where θ and φ are O-Cu-O angles. (**A**) Berry twist mechanism showing, from left to right, the reorientation of the main axis of a square pyramidal configuration by pseudorotations via a trigonal bipyramidal configuration (*24*). The gray atoms in the plane of the trigonal bipyramid are all candidates for becoming apical atoms in a square pyramid. (**B**) Evolution of τ as derived from the first-principles molecular dynamics simulation (window-averaged over an interval of 0.5 ps). The parameter τ describes in a continuous way intermediate configurations of the fivefold-coordinated Cu(II) aqua ion ranging between the regular square pyramidal (τ = 0%) and the regular trigonal bipyramidal (τ = 100%) configurations (*24*).

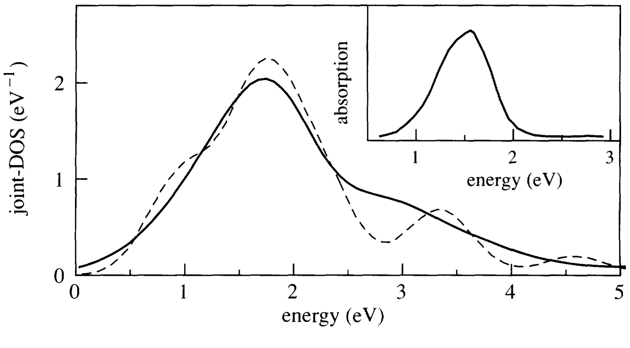

Fig. 3. The joint electronic density of states (DOS) between filled and empty minority spin *d* states (solid curve), averaged over seven instantaneous atomic configurations of the first-principles molecular dynamics simulation, is compared to that for a $Cu(H_2O)_6^{2+}$ cluster (dashed curve). The inset shows the experimental visible near-infrared absorption spectrum (*26*).

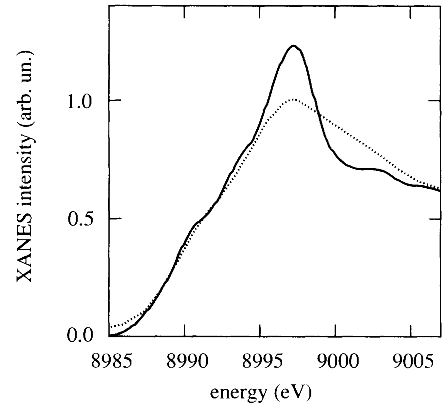

Fig. 4. The theoretical XANES spectrum (solid curve), calculated by considering the density of empty states of *p* symmetry and averaged over eight instantaneous atomic configurations of the first-principles molecular dynamics simulation, is compared to the experimental spectrum (dotted curve) (*7*). The principal peak in the theoretical spectrum has been aligned to the principal experimental peak. Arb. un., arbitrary units.

copper ion with interconversion between square pyramidal and trigonal bipyramidal forms, yielding a water exchange rate of $(5.7 \pm 0.2) \times 10^9\ s^{-1}$, slightly enhanced with respect to the value obtained previously assuming sixfold coordination $[(4.4 \pm 0.1) \times 10^9\ s^{-1}]$ (*15*).

The frequency of occurrence of both five- and sixfold-coordinated Cu(II) ions in crystalline compounds (*24*) suggests that these coordinations are competitive. This work shows that, at variance with the sixfold coordination of cations of similar charge and size such as Ni(II) and Mg(II) (*26*), the Cu(II) aqua ion adopts a fivefold coordination. This is a direct consequence of the $3d^9$ electronic structure of its atomic shell, which causes a departure from octahedral coordination because of the Jahn-Teller effect.

References and Notes

1. E. Ochiai, *Bioinorganic Chemistry, An Introduction* (Allyn & Bacon, Boston, 1977).
2. H. Ohtaki, M. Maeda, *Bull. Chem. Soc. Jpn.* **47**, 2197 (1974).
3. M. Magini, *Inorg. Chem.* **21**, 1535 (1982).
4. G. Licheri *et al.*, *J. Chem. Phys.* **80**, 5308 (1984).
5. T. K. Sham, J. B. Hastings, M. L. Perlman, *Chem. Phys. Lett.* **83**, 391 (1981).
6. Y. Tajiri, H. Wakita, *Bull. Chem. Soc. Jpn.* **59**, 2285 (1986).
7. M. Nomura, T. Yamaguchi, *J. Chem. Phys.* **92**, 6157 (1988).
8. J. Garcia *et al.*, *Chem. Phys.* **132**, 295 (1989).
9. B. Beagley *et al.*, *J. Phys. Condens. Matter* **1**, 2395 (1989).
10. P. S. Salmon, G. W. Neilson, J. E. Enderby, *J. Phys. C Solid State Phys.* **21**, 1335 (1988).
11. P. S. Salmon, G. W. Neilson, *J. Phys. Condens. Matter* **1**, 5291 (1989).
12. S. E. Okan, P. S. Salmon, *Mol. Phys.* **85**, 981 (1995).
13. P. S. Salmon, W. S. Howells, R. Mills, *J. Phys. C Solid State Phys.* **20**, 5727 (1987).
14. R. Poupko, Z. Luz, *J. Chem. Phys.* **57**, 3311 (1972).
15. D. H. Powell, L. Helm, A. E. Merbach, *J. Chem. Phys.* **95**, 9258 (1991).
16. D. H. Powell, G. W. Neilson, J. E. Enderby, *J. Phys. Condens. Matter* **1**, 8721 (1989).
17. ———, *J. Phys. Condens. Matter* **5**, 5723 (1993).
18. R. Car, M. Parrinello, *Phys. Rev. Lett.* **55**, 2471 (1985).
19. A. Pasquarello, K. Laasonen, R. Car, C. Lee, D. Vanderbilt, *Phys. Rev. Lett.* **69**, 1982 (1992).
20. K. Laasonen, A. Pasquarello, R. Car, C. Lee, D. Vanderbilt, *Phys. Rev. B* **47**, 10142 (1993).
21. These solutions were acidified to suppress hydrolysis.
22. J. C. Gallucci, R. E. Gerkin, *Acta Crystallogr.* **C45**, 1279 (1989).
23. The neutron diffraction measurements were carried out at ambient temperature (26°C) using the D4B diffractometer at the Institut Laue-Langevin in Grenoble. The wavelength of the incident neutrons was 0.6991 Å, and the momentum transfer range measured by the diffractometer extended to a maximum value of $Q_{max} \approx 16$ Å^{-1}. In the data reduction, we took the total cross sections for H_2O and D_2O at the incident wavelength from (*32*) and all the other neutron scattering lengths and cross sections from (*33*).
24. B. J. Hathaway, in *Comprehensive Coordination Chemistry*, G. Wilkinson, Ed. (Pergamon, Oxford, 1987), vol. 5, pp. 533–774.
25. Charge neutrality was ensured by adding a uniform background of negative charge. We used a cubic supercell at the experimental density of water. Valence electronic wave functions were expanded on a plane-wave basis set, and core-valence interactions were accounted for by ultrasoft pseudopotentials (*20*). The exchange and correlation energy was described by a generalized gradient approximation (*28*, *29*), which has been shown to give an accurate description for liquid water (*27*, *34*). We used a spin-polarized functional to cope with the open-shell electronic structure in this system.
26. D. T. Richens, *The Chemistry of Aqua Ions* (Wiley, Chichester, UK, 1997).
27. P. L. Silvestrelli, M. Parrinello, *J. Chem. Phys.* **111**, 3572 (1999).
28. A. D. Becke, *Phys. Rev. A* **38**, 3098 (1988).
29. C. Lee, W. Yang, R. G. Parr, *Phys. Rev. B* **37**, 785 (1988).
30. J. Burgess, *Ions in Solution: Basic Principles of Chemical Interactions* (Ellis Horwood, Chichester, UK, 1988), p. 34.
31. S. F. Lincoln, A. E. Merbach, *Adv. Inorg. Chem.* **42**, 1 (1995).
32. D. I. Garber, R. R. Kinsey, *Brookhaven Natl. Lab.* **BNL 325**, 3rd Ed., Vol. II (1976).
33. V. F. Sears, *Neutron News* **3**, 26 (1992).
34. M. Sprik, J. Hutter, M. Parrinello, *J. Chem. Phys.* **105**, 1142 (1996).

35. We thank A. Dal Corso, A. Stirling, and J. C. Wasse for useful interactions. A.P. and D.H.P. acknowledge support from the Swiss National Science Foundation under the program PROFIL. I.P. thanks the University of East Anglia for financial support. Partial support from the Fonds UNIL-EPFL 1997 is acknowledged by the groups at ICMA and IRRMA. The calculations were performed on the NEC-SX4 of the Swiss Center for Scientific Computing.

6 October 2000; accepted 18 December 2000

Observation of All-Metal Aromatic Molecules

Xi Li,[1,2] Aleksey E. Kuznetsov,[3] Hai-Feng Zhang,[1,2]
Alexander I. Boldyrev,[3]* Lai-Sheng Wang[1,2]*

Aromaticity is a concept invented to account for the unusual stability of an important class of organic molecules: the aromatic compounds. Here we report experimental and theoretical evidence of aromaticity in all-metal systems. A series of bimetallic clusters with chemical composition MAl_4^- (M = Li, Na, or Cu), was created and studied with photoelectron spectroscopy and ab initio calculations. All the MAl_4^- species possess a pyramidal structure containing an M^+ cation interacting with a square Al_4^{2-} unit. Ab initio studies indicate that Al_4^{2-} exhibits characteristics of aromaticity with two delocalized π electrons (thus following the 4*n* + 2 electron counting rule) and a square planar structure and maintains its structural and electronic features in all the MAl_4^- complexes. These findings expand the aromaticity concept into the arena of all-metal species.

The name "aromatic compound" was initially bestowed on benzene, its derivatives, and related compounds because of their aroma. Today, the terms "aromatic" and "aromaticity" are used to describe cyclic, planar, and conjugated molecules possessing $(4n + 2)$ π electrons and having specific chemical and structural stability. Despite the undeniable usefulness of the aromaticity concept, it remains controversial and its physical origin is still being debated (*1–3*). Thus, recent years have seen a resurgence in the development of various criteria of aromaticity and in theoretical investigations aimed at gaining a deeper insight into the origin of this phenomenon (*4–8*). In this report, we present experimental and theoretical evidence of aromaticity in an all-metal system: the Al_4^{2-} dianion in a series of bimetallic ionic systems with chemical composition MAl_4^- (M = Li, Na, or Cu). The Al_4^{2-} unit was found to be square planar and to possess two delocalized π electrons, thus conforming to the $(4n + 2)$ electron counting rule for aromaticity.

Using a laser vaporization source and negative ion photoelectron spectroscopy (*9*, *10*), we produced and investigated a series of MAl_4^- clusters (*11*). The negative ion technique affords convenient size selectivity, and photoelectron spectroscopy is quite suitable for providing unique electronic structure information pertaining to the neutral species. We have found that combining photoelectron spectroscopy and ab initio calculations offers a particularly powerful approach to investigating the structure and bonding of novel molecular and cluster species (*12*). Photoelectron spectra of the three MAl_4^- species were measured at two different photon energies. The spectra of the three species are similar (Fig. 1), each with an intense threshold peak (*X* and *A*) followed by two weaker features (*B* and *C*). The *X* and *A* features overlapped heavily and were only resolved in the 355-nm spectrum of $NaAl_4^-$. The vertical electron detachment energies of these features were measured from the peak maxima (Table 1) and compared to the results of the

---

[1] Department of Physics, Washington State University, 2710 University Drive, Richland, WA 99352, USA. [2] W. R. Wiley Environmental Molecular Sciences Laboratory, Pacific Northwest National Laboratory, Mail Stop K8-88, Post Office Box 999, Richland, WA 99352, USA. [3] Department of Chemistry and Biochemistry, Utah State University, Logan, UT 84322, USA.

*To whom correspondence should be addressed. E-mail: boldyrev@cc.usu.edu (A.I.B.); ls.wang@pnl.gov (L.S.W.)